

# Nonlinear Magnetic Reconnection in Low Collisionality Plasmas

M Ottaviani, F Porcelli<sup>1</sup>.

JET Joint Undertaking, Abingdon, Oxon, OX14 3EA.

<sup>1</sup> Politecnico di Torino, Torino, Italy.

**"This document is intended for publication in the open literature. It is made available on the understanding that it may not be further circulated and extracts may not be published prior to publication of the original, without the consent of the Publications Officer, JET Joint Undertaking, Abingdon, Oxon, OX14 3EA, UK".**

**"Enquiries about Copyright and reproduction should be addressed to the Publications Officer, JET Joint Undertaking, Abingdon, Oxon, OX14 3EA".**

**INTRODUCTION.** We discuss magnetic reconnection in collisionless regimes, where electron inertia is responsible for the decoupling of the plasma motion from that of the field lines. These regimes have become relevant in high temperature laboratory plasmas. For example, sawtooth relaxations at JET occur on a time scale shorter than the average collision time. The linear theory of  $m=1$  modes has been recently extended to experimentally relevant regimes [1]. The conclusion from linear theory is that these modes can remain virulent at high temperature, with an initial growth rate,  $\gamma_L$ , which compares favourably with that observed in the experiments. Specifically, it was found that  $\gamma_L \sim \omega_A d$  for  $d > \rho$ ;  $\gamma_L \sim \omega_A d^{1/3} \rho^{2/3}$  for  $d < \rho$ , where  $d = d_e / r_s$ , with  $d_e = c / \omega_{pe}$  the inertial skin depth and  $r_s$  the  $q=1$  radius;  $\rho = \rho_i / r_s$ , with  $\rho_i$  the ion (sound) Larmor radius; and  $\omega_A = L_x / v_A$  is the Alfvén frequency.

Since the linear theory breaks down for very small magnetic island widths, a nonlinear analysis is called for. Recent nonlinear studies [2,3], which assumed that collisionless magnetic reconnection evolves according to a Sweet-Parker process, gave contradicting results.

In this paper, we analyze the behavior of a collisionless, 2-D fluid slab model in the limit  $\rho / d \rightarrow 0$ . Our main result is that, when the island size is larger than the linear layer but smaller than the equilibrium scale length, the reconnection rate exhibits a quasi-explosive time behaviour, during which a current density sub-layer narrower than the skin depth is formed [4].

**THE MODEL.** The equations we solve are

$$\partial_t U + [\varphi, U] = [J, \psi] \quad \text{vorticity equation} \quad (1)$$

$$\partial_t F + [\varphi, F] = 0 \quad \text{inertial Ohm's law} \quad (2)$$

where  $[A, B] \equiv \mathbf{e}_z \cdot \nabla A \times \nabla B$ , with  $\mathbf{e}_z$  the unit vector along the ignorable  $z$  direction ( $\partial_z = 0$ ),  $\varphi$  is the stream function,  $\mathbf{v} = \mathbf{e}_z \times \nabla \varphi$  is the fluid velocity,  $\psi$  is the magnetic flux function,  $U = \nabla^2 \varphi$  is the *fluid vorticity*;  $J = -\nabla^2 \psi$  is the *current density*;  $F \equiv \psi + d^2 J$  is the  *$z$ -canonical momentum*. Eq. (2) implies  $dF/dt = 0$ :  $F$  is conserved on moving fluid elements. The **boundary conditions** are *periodic*. The co-ordinates  $x$  and  $y$  vary in the intervals  $x \in [-L_x, L_x]$  and  $y \in [-L_y, L_y]$ , with the slab aspect ratio  $\varepsilon \equiv L_x / L_y < 1$ . The magnetic field is  $\mathbf{B} = B_0 \mathbf{e}_z + \nabla \psi \times \mathbf{e}_z$ ,  $B_0 = \text{constant}$ . All quantities are dimensionless, with  $L_x = \pi$  and  $\tau_A = (4\pi \rho_m)^{1/2} L_x / B_0$  determining the length and time scale normalisation. At **equilibrium**:  $\varphi_0 = U_0 = 0$ ,  $J_0 = \psi_0 = \cos x$ , and  $F_0 = (1 + d^2) \psi_0$ . The **initial conditions** are the equilibrium plus a small tearing-parity perturbation of the form  $(\varphi, \delta\psi) = \text{Real}\{[\varphi_L(x), \delta\psi_L(x)] e^{i\gamma t + iky}\}$ , with  $k = m\varepsilon$  and  $m$  an integer number. In the limit  $d \ll L_x$ , the solution of the linearized system can be obtained analytically using asymptotic matching techniques. For  $0 < k^2 \leq 1$ , the logarithmic jump of  $\delta\psi_L$  across the reconnecting layers is

$$\Delta' = 2\kappa \tan(\kappa\pi/2), \quad \kappa \equiv (1 - k^2)^{1/2} \quad (3)$$

We are interested in the *large- $\Delta'$*  regime, defined by

$$\Delta' d \geq 1 \quad \Rightarrow \quad \text{macroscopic convection cells, } L_{\text{cell}} \sim L_x. \quad (4)$$

which can be obtained for low values of  $m$  and  $\varepsilon^2 \ll 1$  such that  $\Delta' \sim (8/\pi k^2)$ . In this regime, *the structure of the stream function is macroscopic*, with  $\varphi_L \approx \varphi_\infty \text{sign } x$ ,  $\varphi_\infty \equiv (\dot{\gamma}/k) \psi_\infty$ , everywhere except in narrow layers near the reconnecting surfaces. The current channel in the linear stage has a width  $\delta_L \sim d$ . The linear growth rate is  $\gamma_L \approx kd$ .

**NUMERICAL SOLUTION.** The system of Eqs. (1,2) is solved numerically with a pseudospectral code truncated to  $1024 \times 64$   $(x, y)$  components. We concentrate on the *early nonlinear phase*, specified by the inequalities

$$d < w < 2L_x \quad (5)$$

where  $w$  is the magnetic island width. An important consequence of the inertial Ohm law is that the value of  $F$  at  $x = 0$  is frozen to its initial value, i.e.  $F(x = 0, y, t) = F_0(x = 0) = 1 + d^2$ . The solution shown in Figs. 1-4 has been obtained for  $\varepsilon = 0.5$  and  $d/(2L_x) = 0.04 \Rightarrow d\Delta' \approx 2.03$ .

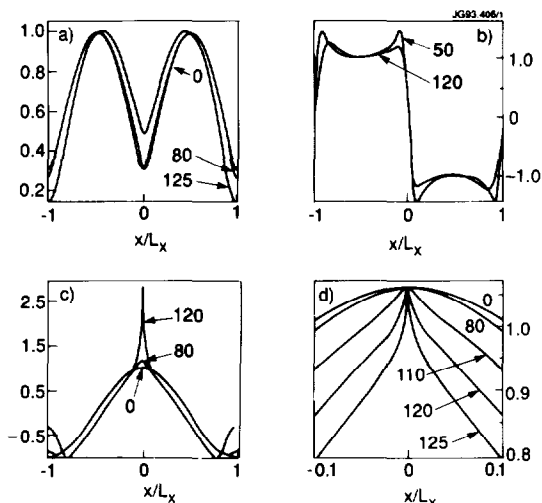


Fig. 1. Cross sections of a) normalized  $\delta\psi$ ; b) normalized  $v_x$ ; c)  $J$ ; d)  $F$  versus  $x$  at  $y=0$  and various times, indicated by arrows.

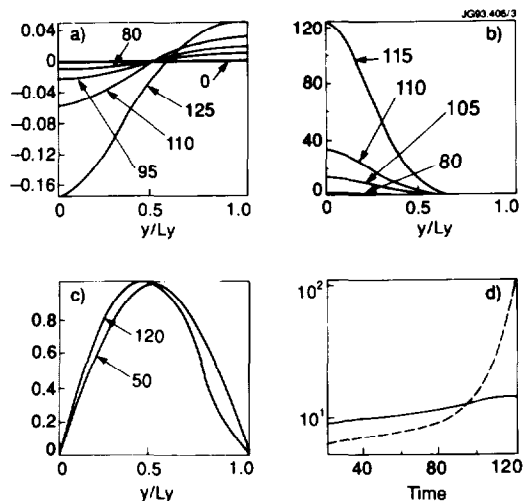


Fig. 2. Cross sections of a)  $\delta\psi$ ; b)  $\partial^2 F / \partial x^2$ ; c) normalized  $v_y$  versus  $y$  at  $x=0$ . Also, d) time dependence of the logarithm of the inverse scale lengths  $\delta_\phi^{-1}$  (solid line) and  $\delta_J^{-1}$  (broken line).

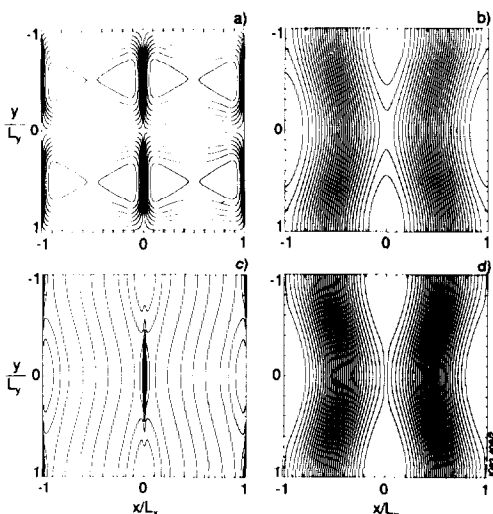


Fig. 3. Contour plots at  $t=120$ : a)  $\phi$ ; b)  $\psi$ ; c)  $J$ ; d)  $F$ .

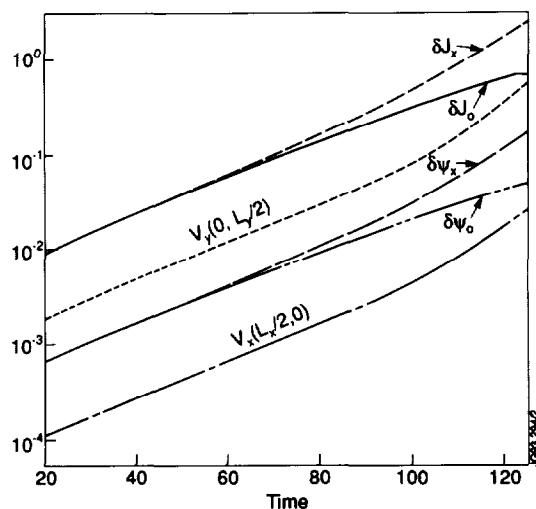


Fig. 4. Time dependence of  $\delta\psi$  and  $\delta J$  at the X- and O-points, of  $v_x(-L_x/2, 0)$  and of  $v_y(0, L_y/2)$ .

**RELEVANT PHENOMENOLOGY.** The linear phase conventionally lasts until  $t \sim 80$ , when the magnetic island reaches a width of order  $d$ . For  $t > 80$ , the width of the profile of  $v_x$ ,  $\delta_\phi \equiv (v_x)_{x=L_x/2} / (\partial_x v_x)_{x=0}$ , as well as that of  $\delta\psi$ , remain of the order of the skin depth (Fig. 1a,b and Fig. 2d). Therefore, the convection cells retain approximately their linear shape well into the nonlinear phase (Fig. 3a). By contrast, the current density profile (Fig. 1c) develops a sub-layer whose width around the X-point,  $\delta_J \equiv (\partial_x^2 \delta J / \delta J)^{-1/2} < d$ , keeps shrinking with time (see also Fig. 2d). This sub-layer is also visible in the profile of  $F$  across the X-point (Fig. 1d). The contraction of this sub-layer is extremely rapid in time, as shown by the graph of  $\partial^2 F / \partial x^2$  versus  $y$  for  $x=0$  and several times in Fig. 2b. Note the development of a current sheet around the reconnection line (Fig. 3c).

Also, note the preservation of the topology of the isolines of  $F$  (Fig. 3d). Finally (Fig. 4) the mode growth remains very rapid throughout the simulation. Indeed, the growth of  $\varphi$ , as well as that of  $\delta\psi$  and  $\delta J$  at the X-points, accelerate in the early nonlinear phase, which is symptomatic of an explosive behaviour (eventually, the mode growth slows down when  $w$  approaches  $L_x$ ).

**ANALYTIC TREATMENT.** The numerical simulations suggest the following *ansatz*:

$$\varphi(x, y, t) = v_o(t)g(x)h(y) + u(x, y, t) \quad (6)$$

where  $h(y) \sim k^{-1} \sin(ky)$ ,  $g(x) \sim \varphi_L(x)/\varphi_\infty$  contains the linear scale length  $d$  and  $u(x, y, t)$  develops the rapid scale length  $\delta(t) \sim \delta_J$  observed in the numerical simulation. The relevant ordering is  $u \ll v_o$  and  $\partial_x u \sim v_o \partial_x g$ . Integration of the collisionless Ohm's law gives  $F = F_o(x_o)$ , where  $x_o(x, y, t) = x - \xi(x, y, t)$  is the initial position of a fluid element situated at  $(x, y)$  at time  $t$  and  $\xi$  is the displacement along the  $x$  direction defined by the equation  $d\xi/dt = v_x$ ,  $\xi(t = -\infty) = 0$ . At  $y = 0$ ,

$$-\int_{x_o}^x dx'/g(x') = \int_{-\infty}^t v_o(t') dt' \equiv \lambda(t). \quad (7)$$

The function  $\lambda(t) > 0$  represents the amplitude of  $\xi$  outside the reconnection layer, where  $g(x) \approx 1$ . In the linear phase,  $-\psi_\infty \approx \lambda < d$ . When  $\lambda > d$ , the magnetic island width  $w \sim 2\lambda$ , so that the early nonlinear phase can also be characterised by the inequality  $d < \lambda < L_x$ , or alternatively  $t_0 < t < t_D$ , with  $\lambda(t_0) \sim d$  and  $t_D$  the characteristic turnover time of the macroscopic eddies in Fig. 3a. Inverting equation (4) in the limit  $d < \lambda < L_x$ , we obtain  $x_o = x_o(x, t)$ , which depends on the time-dependent scale length

$$\delta(t) \equiv d \exp[-\lambda(t)/d]. \quad (8)$$

Thus we see that near the X-point along the  $x$  direction,  $F(x_o)$  (and hence  $J$ ) varies over a distance  $\delta(t)$  which becomes exponentially small in the ratio  $\lambda/d$ . Conversely,  $F$  flattens over a distance  $|x| \sim \lambda$  around the O-point. The formation of a sub-layer is the combined result of the conservation of  $F$  on each fluid element and the flow pattern around the X-point, which acts to increase the local curvature of the  $F$  profile (Fig. 1d). Integrating the equation  $\psi + d^2 J = F$ , where  $J \approx -\partial_x^2 \psi$ , we find that  $\psi$  has an integral structure such that any fine scale variation of  $F$  is smoothed out over a distance  $\sim d$ . Asymptotic evaluation of  $\psi$  at the X- and O-points in the early nonlinear phase gives

$$\psi_X \equiv \psi(0, 0, t) \sim 1 - \frac{1}{2} \lambda^2(t), \quad \psi_O \equiv \psi(0, \pm L_y, t) \sim 1 + \delta(d^2) \quad (9)$$

Now set  $F = F_o(x) + \delta F$ . Then,  $\delta\psi + d^2 \delta J = \delta F$ , and at  $x = 0$ , where  $\delta F = 0$ , we find  $\delta J = -\delta\psi/d^2$ . Thus, an asymmetry develops in the values of  $\delta\psi$  and of  $J$  between the X- and O-points. The spike of the current density at the X-point has an amplitude  $\delta J_X \sim 0.5(\lambda/d)^2$ . Integrating the vorticity equation over the quadrant  $S: [0 \leq x \leq L_x, 0 \leq y \leq L_y]$  gives

$$\partial_t \int_S U dx dy = \oint_C J d\psi. \quad (10)$$

where  $C$  is the boundary of  $S$ . With the *ansatz* (6), and neglecting corrections  $\mathcal{O}(k^2 d^2)$  contributed by  $\partial_y^2 \varphi$ , we find

$$\partial_t \int_S (\partial_x^2 \varphi) dx dy \approx -(4c/k^2 d) d^2 \lambda/dt^2, \quad (11)$$

where  $c > 0$  is a factor of order unity, which depends weakly on time (e.g.  $1 \leq c \leq 1.4$  in Fig. 2d). The dominant contribution from the r.h.s. of Eq. (10) is

$$\oint_C J d\psi \approx \delta\psi_X - \delta\psi_O - (\delta\psi_X^2 - \delta\psi_O^2)/2d^2 \quad (12)$$

Finally, using an interpolation formula between the linear and early nonlinear limits of the r.h.s. of (12), we obtain an equation for the evolution of  $\hat{\lambda}(t) \equiv \lambda(t)/d$ :

$$d^2 \hat{\lambda}/dt^2 \approx \hat{\lambda} + c_2 \hat{\lambda}^4 \quad (13)$$

where  $\hat{t} \equiv \gamma_L t$  and  $c_2 \approx 1/16c > 0$  can be taken constant. The solution is  $\hat{\lambda}(\hat{t}) = \left[ \frac{(1-\alpha)}{(1-\alpha e^{3\hat{t}})} \right] e^{\hat{t}}$ , where  $\alpha = \beta - (\beta^2 - 1)^{1/2}$ ,  $\beta = 1 + 5/c_2$ , and we have chosen the time origin so that  $\hat{\lambda}(0) \equiv 1$ . Thus, once the early nonlinear regime is entered,  $\lambda(t)$  accelerates and reaches a macroscopic size over a fraction  $\sim \ln(\alpha^{-1/3})$  of the linear growth time. Eventually, we can expect this quasi-explosive growth to cease as  $\lambda$  approaches  $L_x$ .

**DISCUSSION AND CONCLUSIONS.** Collisionless reconnection in regimes where the instability parameter  $\Delta'$  is large and global convection cells develop does not follow the standard Sweet-Parker scenario [5-7]. In

this context, we note a fundamental difference in the nonlinear flow pattern between the collisionless case (Fig. 3) and the resistive case (Fig. 5). The Sweet-Parker scenario applies to the regime  $\eta^{1/2} \gg d$ , where  $\eta$  is the normalized resistivity (inverse Reynolds' number). It is of interest to study the limit  $\eta^{1/2} \ll d \ll \eta^{1/3}$ . In this regime, the linear phase is dominated by exponential evolution with the resistive growth rate  $\gamma_L \sim \eta^{1/3} \omega_A$ . During an initial nonlinear phase, where  $\eta^{1/3} < \lambda < \eta/d^2$ , the displacement  $\lambda$  grows algebraically in time,  $\lambda \sim \eta t^2$ , while the width of the current channel shrinks from  $\delta_L \sim \eta^{1/3}$  to  $\delta \sim (\eta/\lambda)^{1/2}$ . This initial nonlinear regime is consistent with Sweet-Parker. When  $\lambda \sim \eta/d^2$ , also  $\delta \sim d$ . Therefore, the initial nonlinear behavior must change for  $\lambda > \eta/d^2$ , as for these values of  $\lambda$  the current in the layer is distributed mostly over a distance  $\sim d$ , independently of  $\lambda$ . Assuming that the formation of the current spike (cf Eq. 10) is impeded (see below), we can expect a resumption of exponential growth in this later nonlinear phase, with  $\lambda \propto \exp(d \cdot t)$ .

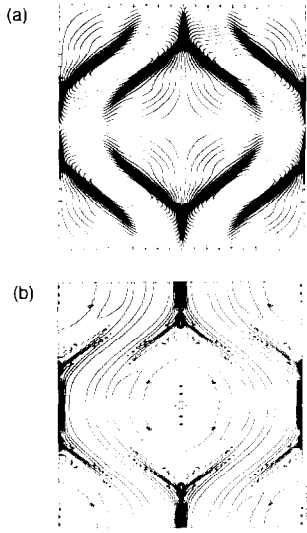


Fig. 5 Contour plots of a) the stream function  $\phi$  and b) the current density  $J$  in the resistive case.

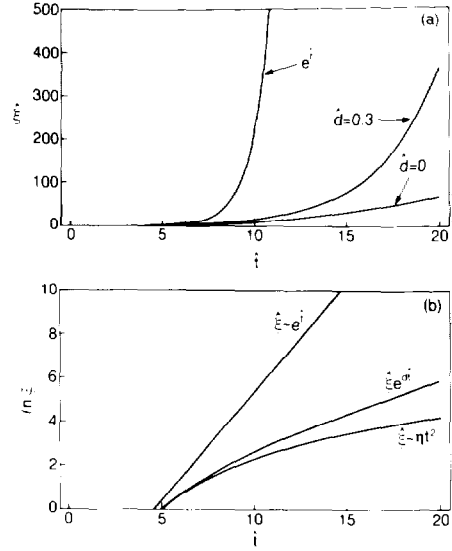


Fig. 6 Time evolution of the normalized displacement  $\hat{\xi} = \lambda / \eta^{1/3}$  in the regime  $\eta^{1/2} \ll d \ll \eta^{1/3}$ : a) linear plot; b) semi-log plot.

This behavior can be summarized by the following phenomenological equation for  $\xi \equiv \lambda / \eta^{1/3}$ :

$$d\hat{\xi}/d\hat{t} = \left[ (1 + \hat{d}^2 \hat{\xi}) / (1 + \hat{\xi}) \right]^{1/2} \hat{\xi} \quad (14)$$

where  $\hat{t} = \eta^{1/3} t$  and  $\hat{d} = d / \eta^{1/3}$ . The numerical solution of Eq. (14) is shown in Fig. 6. The growth eventually saturates when the displacement reaches a macroscopic size ( $\lambda \sim L_{cell}$ ). One expects that the current spike will be limited by effects not taken into account by the present analysis. Such effects may include collisions (most notably, electron viscosity), velocity-space instability associated with the current density gradient, 3-D effects, etc. Further work needs to be done to determine the relevant effects for interesting applications. While the current spike is being formed, the reconnection rate exhibits a quasi-explosive time behavior. Physically, the flow rotation accelerates following the intensification of the electromagnetic torque  $\oint_C \mathbf{J} \times \mathbf{B} \cdot d\mathbf{l} = \oint_C J d\psi$  in the early nonlinear regime. This torque is mainly contributed by the average  $J_z B_x$  force between the X- and O-points within a magnetic island.

In conclusion, we believe that the inclusion of the electron inertial term in Ohm's law opens the possibility to understand the rapidity of relaxation processes observed in low collisionality plasmas.

**REFERENCES** [1] F.Porcelli, Phys. Rev. Lett. **66**, 425 (1991). [2] J.Wesson, Nuclear Fusion **30**, 2545 (1990). [3] J.F.Drake and R.G.Kleva, Phys. Rev. Lett. **66**, 1458 (1991). [4] M. Ottaviani and F. Porcelli, Phys. Rev. Lett. **71**, 3802 (1993). [5] P.A.Sweet, in *Electromagnetic Phenomena in Cosmic Physics*, ed. by B.Lehnert (Cambridge University Press, 1958), p. 123. [6] E.N.Parker, J. Geophys. Research **62**, 509 (1957). [7] B.B.Kadomtsev, Fiz. Plasmy **1**, 710 (1975) [Sov. J. Plasma Phys. **1**, 389 (1975)].